THE JOURNAL OF PHYSICAL CHEMISTRY B

Article

pubs.acs.org/JPCB

Heterogeneous Nucleation of Giant Bubbles from a Langmuir Monolayer in a Laser Focus

Jürgen Gewinner and Thomas M. Fischer*

Institut für Experimentalphysik, Universität Bayreuth, 95440 Bayreuth, Germany

Supporting Information

ABSTRACT: Evidence is shown that spherical structures of methyloctadecaoate nucleated from a Langmuir monolayer in a laser focus are giant multilamellar bubbles. The bubbles remain stable in the laser focus but respread to the monolayer outside of the focus. Bubbles coalesce when brought into contact. The coalescence is accompanied by a volume increase and area decrease of the fused bubble as compared to the original pair of bubbles. Bubbles deviate from spherical and are compressed along the flow direction of the surrounding monolayer when they are advected versus and trapped at phase boundaries of the monolayer.

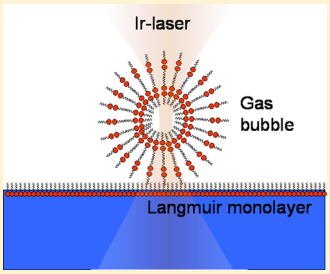

INTRODUCTION

Langmuir monolayers at the air−water interface exhibit a rich variety of different phases as a function of their surface density and as a function of temperature.[1] Their insolubility in both polar and apolar liquids usually forces them to remain at the air−water interface and avoid the bulk of the water. However, compression beyond the equilibrium spreading pressure renders the interfacial arrangement of the molecules metastable. As a result the rate of formation of three-dimensional structures on top or below the monolayer increases with the amount of supercompression of the film. The resulting collapse structures seem to depend on the monolayer equilibrium phases prior to collapse, and they vary with the compression rate. They therefore also depend on transport properties such as the viscoelastic properties of the film. The collapse structures might consist of bilayers formed on top of the monolayer[2] or by structures that form in the water below the monolayer. Folds,[3] tubes,[4] buds,[5] or small vesicles,[6,7] but also irregular structures[8] are examples of structures forming at the aqueous side of the collapsing monolayer. These structures can be reversibly or irreversibly nucleated upon compression. Reversible collapse is a very important mechanism occurring at the gas-exchange interface in the lung−alveoli during the breathing cycle. This has not only triggered the experimental research on monolayer collapse but has also led to the theoretical work of Lu et al.[9] and to simulations by Baoukina et al.[10] of monolayer collapse. Lu et al.[9] could show that the formation of elliptical folds occurs at surface pressures far below the surface tension of water because of the binding energy between the leaflets of the bilayers within the fold. Baoukina et al.[10] used simulations to confirm these findings but also to predict the formation of semivesicles remaining bound to the monolayer or to detached full vesicles. Recent theoretical work has suggested folds of shapes modulated along the fold by a soft Goldstone mode.[11]

On a macroscopic scale, nucleation of collapse structures is homogeneous because the same thermodynamic conditions hold throughout the entire monolayer. Microscopic techniques reveal only a small region of the entire monolayer. Collapse generically happens outside of the field of view and can be visualized only indirectly from intermittent jerks observed in the motion of the monolayer in the field of view.[12,13] However, the pioneering work of Angelova, Vollhard, and Ionov[8] showed that collapse structures preferentially nucleate at the border of condensed monolayer domains. Hence, on a mesoscopic scale, nucleation is heterogeneous. This brings about the idea to heterogeneously induce the nucleation of monolayer collapse by locally perturbing the monolayer at a single well-defined location.

Vesicles are the most symmetric among all collapse structures. They can be formed by more efficient mechanisms than monolayer collapse and have been investigated intensely. When put under stress, vesicles may connect to other structures via tubes[14−16] that coexist with the vesicles under equilibrium conditions. Bubbles are the analogue of vesicles on the gaseous side of the air−water interface. Soap bubbles are common structures forming from the aqueous phase when soluble surfactants are present. Circular bubbles of thermotropic smectic liquid crystals are bubbles formed in the absence of water from water-insoluble molecules.[17−20] The formation of bubbles from water-insoluble surfactants on the other hand is less common.

The aim of this work is to present a new technique that allows nucleating collapse structures in the focus of a laser positioned in the field of view of the microscope. An analysis of the intensity profile, coalescence behavior, and hydrodynamic flow of the spherical collapse structures lets us conclude that the collapse structure is an insoluble surfactant bubble that remains connected to the monolayer rather than a vesicle.

Received: July 23, 2013
Revised: October 25, 2013
Published: November 7, 2013

dx.doi.org/10.1021/jp407291a | J. Phys. Chem. B 2013, 117, 14749−14753

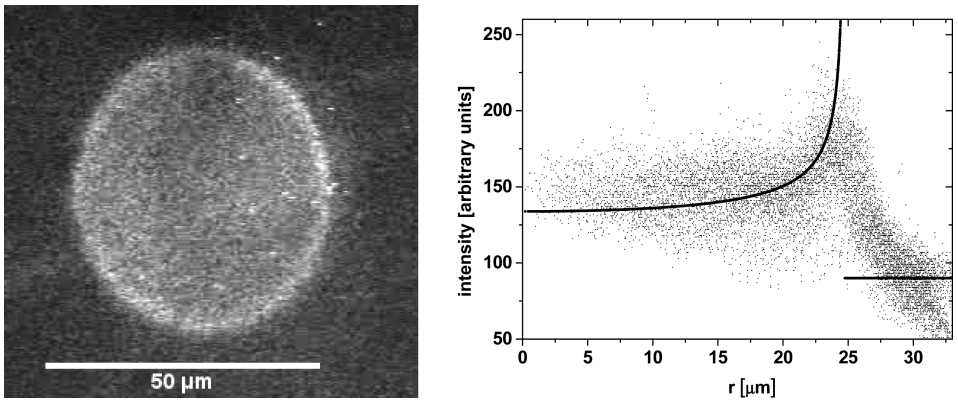

Figure 1. (left) Fluoresence microscopy image of a circular collapse structure observed near the laser focus. (right) Intensity profile of the structure to the left. The solid line is a fit with the intensity profile of a spherical shell plus a background noise intensity. A video (jp407291a_si_001.mpg) of the nucleation process of the structure is provided in the Supporting Information.

MATERIALS AND METHODS

Methyloctadecanoate was purchased from Sigma Aldrich. The surfactant was dissolved in chloroform (about 1 mM) and fluorescently labeled with 1 mol of 1,2-dihexadecanoyl-*sn*-glycero-3-phosphoethanolamine and triethylammonium salt (Texas Red DHPE) purchased from Molecular Probes (Eugene, Oregon, U.S.A.). The surfactant was spread at the air−water interface. The subphase was pure water (Millipore Milli-Q 18 MΩ cm). The setup for studying collapse phenomena has been described in detail elsewhere.[21] Briefly, it consists of a home-built Langmuir trough placed on the stage of an inverted fluorescence microscope (Zeiss-Axiovert 135) with a 100× water immersive objective. The temperature of the trough can be controlled precisely. An IR laser beam (λ = 1064 nm, P = 2 mW−10 W) was used to locally heat the monolayer in the focus of the objective. The light is partially absorbed by the subphase and heats the monolayer locally around the focus.

RESULTS

In previous work,[22,23] it was observed that upon focusing an IR laser on a methyloctadecanoate monolayer in the liquid condensed phase, at a laser power higher than a critical value of about 2 W, a radial thermocapillary flow of the surface toward the center sets in, resulting in local collapse of the monolayer. The collapse structure in methyloctadecanoate depends on the surface temperature, surface pressure, and laser power of the IR laser. Here, we focus on spherical structures forming upon collapse and show that they are bubbles tethered to the monolayer.

Our experiments are performed at an area per molecule below 19 Å^2/molecule and at a temperature of T = 28 °C. At these conditions, the monolayer has already globally collapsed via cracks; however, no homogeneous nucleation of 3d structures is observed in the field of view with the fluorescence microscope. Upon increasing the IR laser power beyond the threshold power of $P_c \approx 2$ W, we observe a radial inward flow of the monolayer toward the laser focus. When we decrease the area per molecule, the threshold power for collapse usually decreases. Collapse structures occur at high laser powers and low area per molecule. In the center, three-dimensional aggregates form, which coexist with highly symmetric circular structures. In the left part of Figure 1, we show a fluorescence microscope image of such a circular structure. The measured intensity profile of the circular structure is plotted versus the lateral distance from the center of the circular structure on the right-hand side of Figure 2. For a spherical shell of radius R of a randomly oriented fluorescence dye, we would expect an intensity profile $I(x,y) \propto (R^2 - x^2 - y^2)^{-1/2}$ because the fluorescence light eminates only from the shell of the sphere and not from the interior of the sphere. The solid line in the figure corresponds to such an intensity profile. We observe circular collapse structures with radii ranging from 1 to 40 μm.

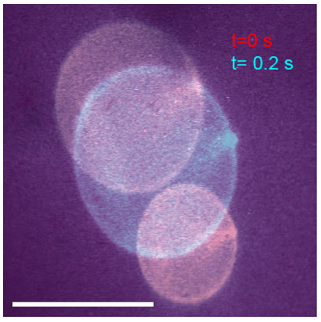

Figure 2. Superposition of two fluorescence microscope images of two spherical collapse structures (red) just prior to coalescence and the resulting structure (blue) after coalescence. The scale bar is 50 μm. A video (jp407291a_si_002.mpg) of the coalescence is provided in the Supporting Information.

It is possible to nucleate two or more spherical collapse structures in the laser focus. A collection of two spheres (colored red) is shown in Figure 2. Eventually, two spheres of radii R_{1i} and R_{2i} coalesce to form a third single spherical structure of radius R_f (colored blue). Assuming a spherical shape of the particle, we can compute the area $A = 4\pi R^2$ and volume $V = 4\pi/3R^3$. We observe an increase of volume $\Delta V/V = (V_f - V_{1i} - V_{2i})/V_f \approx 10\% \pm 7\%$ upon fusion, while the absolute area shrinks $\Delta A/A = (A_f - A_{1i} - A_{2i})/A_f \approx -10\% \pm 7\%$. Figure 2 shows two spheres prior to coalescence (red) and the resulting final single sphere (blue).

When we decrease the laser power, surfactant molecules leave the surface of the sphere and are respread to the monolayer. In Figure 3, we show fluorescence images of the respreading when the laser power is reduced. A corona of respread monolayer surrounds the spherical object.

Tethering and Resistance to Flow. The monolayer in the focus of the IR laser is often subject to characteristic flow. The flow profile of the monolayer can be tracked via the texture of

dx.doi.org/10.1021/jp407291a | J. Phys. Chem. B 2013, 117, 14749−14753

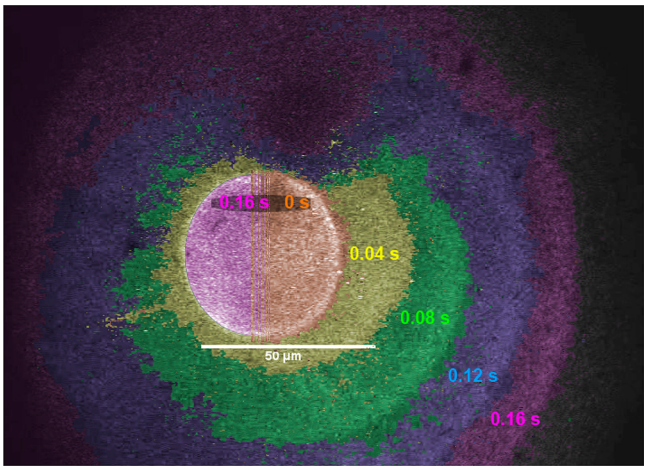

Figure 3. Superposition of fluorescence images of a spherical collapse structure for different lag times after reducing the laser power (different times are colored differently). No monolayer has respreads right after the reduction (brown), a growing corona of the respreading monolayer surrounds the spherical structure as time progresses, while the size of the spherical structure shrinks a little (pink). A video (jp407291a_si_003.mpg) of the monolayer expulsion is provided in the Supporting Information.

the monolayer. In Figure 4, we depict the monolayer and several nucleated three-dimensional spherical structures resid-

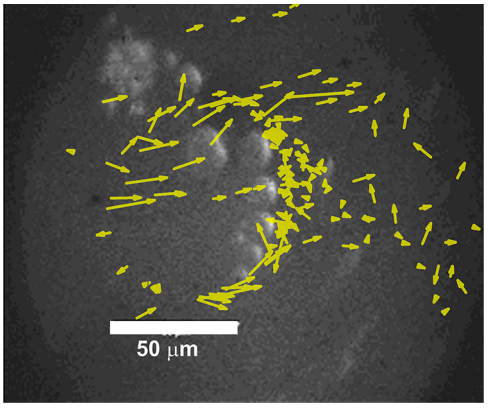

Figure 4. Spherical collapse structures stationary positioned inside of the flow of the surrounding monolayer. The collapse structure are darker at the front facing the flow than that at the rear. The scale bar is 50 μm. A video (jp407291a_si_004.mpg) of the collapse structures in the flow is provided in the Supporting Information.

ing in the flow. The two-dimensional flow profile is shown as yellow arrows and resembles that of capillary flow around a two-dimensional melted gaseous domain recently observed by Muruganathan et al.[24] The spherical structures are stationary and located at the rear of the melted moving phase close to the boundary to the quiescent monolayer phase. It is evident that the spherical structures are brighter at their rear than at the front that faces the surrounding monolayer flow.

DISCUSSION

From Figure 1, we conclude that the circular object is a spherical shell of insoluble surfactants. In principle, it could be either a vesicle or a bubble. In one case, the interior lipid monolayer would be oriented with the head groups toward the internal aqueous phase. If the spherical shell is an air-filled bubble, the interior monolayer of the bubble would be oriented with the alkyl chains toward the air. We find it difficult to explain the volume increase if the spherical objects are vesicles. If the spherical objects are bubbles, our reasoning is as follows. Bubbles cannot be created without the IR laser because without the laser, it is not possible to create sufficient internal pressure in the bubble interior to stabilize the bubble. We hence assume that the internal pressure in a bubble is the air pressure inside of the gas bubble plus an additional pressure created by the laser

$$p_i = p_i^{\text{air}} + p^{\text{laser}} \tag{1}$$

In mechanical equilibrium, the internal pressure is balanced by the outside air pressure p_o^{air} plus the Laplace pressure produced by the lipid film of the bubble

$$p_i = p_o^{\text{air}} + \frac{4\sigma}{R} \tag{2}$$

Here, σ denotes the interfacial tension of one side of the bubble film, and R is the radius of the bubble. When the bubble is nucleated by the laser, the inside air pressure initially cannot exceed the outside air pressure, and we can estimate the laser pressure necessary for nucleation of the bubbles by the Laplace pressure in the smallest bubbles observed.

$$p^{\text{laser}} \approx \frac{4\sigma}{R_{\text{min}}} \tag{3}$$

Here, $R_{\text{min}} \approx 1$ μm is the smallest radius of bubbles observed in the experiment. We assume that the inside air is at a constant temperature, and an ideal gas behavior

$$p_i^{\text{air}} V_i = NkT \tag{4}$$

holds for the air inside of the bubble.

Upon coalescence, we assume both bubbles to be impermeable for the air of the outside, such that the number of air molecules in the final bubble equals the number of air molecules inside of the initial pair of bubbles, and

$$p_{i,1i}^{\text{air}} V_{1i} + p_{i,2i}^{\text{air}} V_{2i} = p_{i,f}^{\text{air}} V_f \tag{5}$$

where we have indices i1,i2 for the initial bubbles and f for the final bubble. Because the radius of the final bubble is larger than that of the initial bubble, the inside pressure will be reduced by the decrease of the Laplace pressure such that the inside air can expand.

Inserting eqs 1−4 into eq 5, we arrive at

$$\left(p_0^{\text{air}} + \frac{4\sigma}{R_{1i}} - \frac{4\sigma}{R_{\text{min}}}\right)V_{1i} + \left(p_0^{\text{air}} + \frac{4\sigma}{R_{2i}} - \frac{4\sigma}{R_{\text{min}}}\right)V_{2i} = \left(p_0^{\text{air}} + \frac{4\sigma}{R_f} - \frac{4\sigma}{R_{\text{min}}}\right)V_f \tag{6}$$

Resolving eq 6 for the interfacial tension, we find

$$\sigma = \frac{p_0^{\text{air}} R_{\text{min}}}{4} \frac{1}{\left(1 - \frac{\Delta A R_{\text{min}}}{3\Delta V}\right)} \tag{7}$$

The quantities on the right-hand side can be extracted from the experiments, and we find an interfacial tension of $\sigma \approx 25$ mN/m of the surfactant−air interface corresponding to a surface pressure of roughly $\pi \approx 50$ mN/m that corresponds reasonably well with the collapse pressure $\pi_c \approx 40$ mN/m of the methyloctadecanoate monolayer at the air−water interface.[25]

dx.doi.org/10.1021/jp407291a | J. Phys. Chem. B 2013, 117, 14749−14753

Figure 5 shows the surface tension extracted from the experiments as a function of the coalesced bubble.

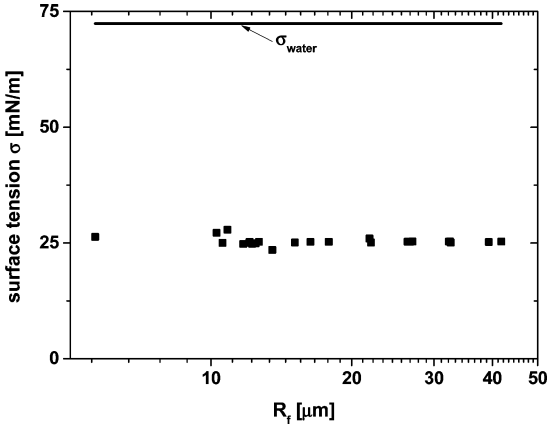

Figure 5. Surface tension of the bubbles versus the radius of the final bubble computed from the volume changes and area changes upon coalescence of the two initial bubbles.

When the laser is shut off, the bubble acts a reservoir for the monolayer, the surfactants are respread to the monolayer at the air−water interface, and we observe a respread surface (Figure 3) that exceeds the area $A_f = \pi R_f^2$ of the bubble without significant reduction in size of the bubble. We conclude that the bubble consists of a multilamellar film of insoluble surfactants.

The fact that the bubble can be deformed by flow shows that the bubble is not stress-free but must be still in contact with the water−air surface. It also shows that there is a monolayer phase in the center of the focus that is fixed to the laser focus while the surrounding monolayer flows around this phase and tries to pull the central phase with the flow. However, it does not succeed in doing so because the viscous forces of the flow are balanced by a force exerted by the laser. The three-dimensional bubbles must be fixed to the stationary phase and are hence in contact with the monolayer. The fluorescence intensity gradient from the front toward the rear proves the multilamellar character of the three-dimensional bubble. More lamellae must be present at the rear of the bubble than at the front, and the number of bilayers forming the bubble film is not constant across the bubble.

CONCLUSIONS

In conclusion, we have proven that the circular collapse structure is a multilamellar bubble filled with air by the IR laser that is connected to the air−water interface. The bubble is stable only in the presence of the laser and is successively stripped of bilayers when the laser power is reduced. The bubble consists of a multilamellar bilayer of surfactants, and defects in the bilayers can be produced by viscous forces that lead to bubbles with different numbers of bilayers in the front as compared to those in the rear of the bubble.

ASSOCIATED CONTENT

Supporting Information

Videos of the nucleation process of the structure (jp407291a_si_001.mpg), the coalescence (jp407291a_si_002.mpg), the monolayer expulsion (jp407291a_si_003.mpg), and the collapse structures in the flow (jp407291a_si_004.mpg). This material is available free of charge via the Internet at http://pubs.acs.org.

AUTHOR INFORMATION

Corresponding Author

*E-mail: thomas.fischer@uni-bayreuth.de.

Notes

The authors declare no competing financial interest.

ACKNOWLEDGMENTS

This work has been supported by the German Science Foundation via Grant Fi 548/11-1

REFERENCES

(1) Kaganer, V. M.; Möhwald, H.; Dutta, P. Structure and Phase Transitions in Langmuir Monolayers. *Rev. Mod. Phys.* **1999**, *71*, 779−819.

(2) Ries, H. E., Jr. Stable Ridges in a Collapsing Monolayer. *Nature* **1979**, *281*, 287−289.

(3) Ybert, C.; Lu, W.; Möller, G.; Knobler, C. M. Collapse of a Monolayer by Three Mechanisms. *J. Phys. Chem. B.* **2002**, *106*, 2004−2008.

(4) Lee, K. Y. C. Collapse Mechanism of Langmuir Monolayers. *Annu. Rev. Phys. Chem.* **2008**, *59*, 771−791.

(5) Schief, W. R.; Touryan, L.; Hall, S. B.; Vogel, V. Nanoscale Topographic Instabilities of a Phospholipid Monolayer. *J. Phys. Chem. B* **2000**, *104*, 10444−10444.

(6) Schief, W. R.; Hall, S. B.; Vogel, V. Spatially Patterned Static Roughness Superimposed on Thermal Roughness in a Condensed Phospholipid Monolayer. *Phys. Rev. E* **2000**, *62*, 6831−6837.

(7) Gopal, A.; Lee, K. Y. C. Morphology and Collapse Transition in Binary Phospholipid Monolayers. *J. Phys. Chem. B* **2001**, *105*, 10348−10354.

(8) Angelova, A.; Vollhardt, D.; Ionov, R. 2D−3D Transformations of Amphiphilic Monolayers Influenced by Intermolecular Interactions: A Brewster Angle Microscopy Study. *J. Phys. Chem.* **1996**, *100*, 10710−10720.

(9) Lu, W.; Knobler, C. M.; Bruinsma, R. F.; Twardos, M.; Dennin, M. Folding Langmuir Monolayers. *Phys. Rev. Lett.* **2002**, *89*, 146107/1−146107/4.

(10) Baoukina, S.; Monticelli, L.; Risselada, H. J.; Siewert, L.; Marrink, J.; Tieleman, D. P. The Molecular Mechanism of Lipid Monolayer Collapse. *Proc. Natl. Acad. Sci. U.S.A.* **2008**, *105*, 10803−10808.

(11) Diamant, H.; Witten, T. A. Shape and Symmetry of a Fluid-Supported Elastic Sheet. *Phys. Rev. E.* **2013**, *88*, 012401/1−012401/8.

(12) Hatta, E.; Fischer, Th. M. Modulation Crack Growth and Crack Coalescence upon Langmuir Monolayer Collapse J. *Phys. Chem. B* **2002**, *106*, 589−592.

(13) Gopal, A.; Belyi, V. A.; Diamant, H.; Witten, T. A.; Lee, K. Y. C. Microscopic Folds and Macroscopic Jerks in Compressed Lipid Monolayers. *J. Phys. Chem. B* **2006**, *110*, 10220−10223.

(14) (a) Waugh, R. E. Surface Viscosity Measurements from Large Bilayer Vesicle Tether Formation. I. Analysis. *Biophys. J.* **1982**, *38*, 19−27. (b) Waugh, R. E. Surface Viscosity Measurements from Large Bilayer Vesicle Tether Formation. II. Experiment. *Biophys. J.* **1982**, *38*, 29−37.

(15) Bozic, B.; Svetina, S.; Zeks, B.; Waugh, R. E. Role of Lamellar Membrane Structure in Tether Formation from Bilayer Vesicles. *Biophys. J.* **1992**, *61*, 963−973.

(16) Rossier, O.; Cuvelier, D.; Borghi, N.; Puech, P. H.; Derényi, I.; Buguin, A.; Nassoy, P.; Brochard-Wyart, F. Giant Vesicles under Flows: Extrusion and Retraction of Tubes. *Langmuir* **2003**, *19*, 575−584.

(17) Stannarius, R.; Cramer, C. Surface Tension Measurements in Freely Suspended Bubbles of Thermotropic Smectic Liquid Crystals. *Liq. Cryst.* **1997**, *23*, 371−375.

(18) Harth, K.; Stannarius, R. Measurement of the Interface Tension of Smectic Membranes in Water. *Phys. Chem. Chem. Phys.* **2013**, *15*, 7204−7209.
(19) May, K.; Harth, K.; Trittel, T.; Stannarius, R. Dynamics of Freely Floating Smectic Bubbles. *Eur. Phys. Lett.* **2012**, *100*, 16003/1−16003/6.
(20) Ishii, Y.; Tabe, Y. Gas Permeation of LC Films Observed by Smectic Bubble Expansion. *Eur. Phys. J. E* **2009**, *30*, 257−264.
(21) Wurlitzer, S.; Lautz, C.; Liley, M.; Duschl, C.; Fischer, Th. M. Mircromanipulation of Langmuir-Monolayers with Optical Tweezers. *J. Phys. Chem. B* **2001**, *105*, 182−187.
(22) Muruganathan, R. M.; Fischer, Th. M. Laser Induced Local Collapse in a Langmuir Monolayer. *J. Phys. Chem. B* **2006**, *110*, 22160−22165.
(23) Aliaskarisohi, S.; Fischer, Th. M.; Wilke, N. Dilatational Yielding of Solid Langmuir Monolayers. *J. Phys. Chem. B* **2011**, *115*, 11631−11637.
(24) Muruganathan, R. M.; Khattari, Z.; Fischer, Th. M. Non-equilibrium Bubbles in a Flowing Langmuir Monolayer. *J. Phys. Chem. B* **2005**, *109*, 21772−21778.
(25) Lundquist, M. Relation Between Polymorphism in 2-Dimensional Monomolecular Films on Water to Polymorphism in 3-Dimensional State, and Formation of Multimolecular Films on Water 3. Ethyl Esters of Aliphytic Acids. *Chem. Scr.* **1971**, *1*, 197−209.